Assimilating summer sea-ice thickness observations improves Arctic sea-ice forecast

Ruizhe Song[1,2,3,4], Longjiang Mu[2], Svetlana N. Loza[3,5], Frank Kauker[3], Xianyao Chen[1,2]

[1]Frontier Science Center for Deep Ocean Multispheres and Earth System and Physical Oceanography Laboratory, Ocean University of China, Qingdao, China
[2]Laoshan Laboratory, Qingdao, China
[3]Alfred Wegener Institute, Helmholtz Centre for Polar and Marine Research, Bremerhaven, Germany
[4]Academy of the Future Ocean, Ocean University of China, Qingdao, China
[5]Shirshov Institute of Oceanology, Russian Academy of Sciences, Moscow, Russia

Key Points:

- Assimilating summer CryoSat-2 sea-ice thickness (SIT) observations makes more skillful Arctic ice-edge forecasts on multiple time scales.
- The long-term SIT forecasts improve with the assimilation of summer CryoSat-2 SIT observations.
- Further refinement is needed for summer CryoSat-2 SIT observations.

Corresponding author: Longjiang Mu, `ljmu@qnlm.ac`

Abstract

Accurate Arctic sea-ice forecasting for the melt season is still a major challenge because of the lack of reliable pan-Arctic summer sea-ice thickness (SIT) data. A new summer CryoSat-2 SIT observation dataset based on an artificial intelligence algorithm may alleviate this situation. We assess the impact of this new dataset on the initialization of sea-ice forecasts in the melt seasons of 2015 and 2016 in a coupled sea ice-ocean model with data assimilation. We find that the assimilation of the summer CryoSat-2 SIT observations can reduce the summer ice-edge forecast error. Further, adding SIT observations to an established forecast system with sea-ice concentration assimilation leads to more realistic short-term summer ice-edge forecasts in the Arctic Pacific sector. The long-term Arctic-wide SIT prediction is also improved. In spite of remaining uncertainties, summer CryoSat-2 SIT observations have the potential to improve Arctic sea-ice forecast on multiple time scales.

Plain Language Summary

Arctic sea ice is rapidly declining due to global warming, especially in summer. Accurate sea-ice forecasting is important to understand the potential influence of these changes and devise effective responses. The performance of sea-ice forecasts highly depends on the accuracy of the initial sea-ice states. So refining the initial conditions of sea-ice forecasts with satellite observations is a common way to reduce forecast errors. However, obtaining reliable summer pan-Arctic satellite sea-ice thickness (SIT) data is challenging due to complex ice-surface conditions in summer. A new artificial-intelligence-based summer SIT satellite data product may improve initial SIT states. We integrate this dataset into a sea-ice forecast system to evaluate its impact on forecast skill. We find that the new summer satellite SIT data can reduce short-term ice-edge location forecast errors and benefit long-term SIT forecasts.

1 Introduction

Arctic sea ice is declining at unprecedented speed (Rothrock et al., 1999; Comiso et al., 2008; Kwok & Rothrock, 2009; Stroeve et al., 2012), which would pose challenges to climatic and ecological stakeholders (Landrum & Holland, 2020). The Arctic Passage, opening up with the gradually melting summer sea ice, calls for accurate Arctic sea-ice prediction from daily to seasonal scales for safe navigation (Jung et al., 2016).

Accurate initialization of sea-ice state is vital for predicting Arctic sea ice (e.g., Blanchard-Wrigglesworth et al., 2011; Guemas et al., 2016; Xie et al., 2016; Dirkson et al., 2017; Bushuk et al., 2022). The assimilation of sea-ice concentration (SIC) has improved the short-term sea-ice forecasts greatly as documented in the literature, and is now widely used at forecasting centers (e.g., Hebert et al., 2015; Lemieux et al., 2015). Sea-ice thickness (SIT) persists longer, therefore assimilation of SIT raises long-term sea-ice forecast skills even higher (Day, Hawkins, & Tietsche, 2014; Shu et al., 2021; Mu et al., 2022).

However, the potential impacts of summer SIT observations on sea-ice forecasts are not examined comprehensively yet due to a lack of data. An effective retrieval method for the remotely sensed SIT from May to September was desired (Laxon et al., 2013; Ricker et al., 2014). The complex summer ice-surface conditions restrict the application of classical algorithms designed for winter conditions. For instance, melt ponds which occupy a huge fraction of the sea-ice surface in the melt seasons (Maykut et al., 1992) complicate the classification algorithms (Lee et al., 2018; Tilling et al., 2019) and introduce large uncertainties due to increased moisture in the snow (Drinkwater, 1991). On the other hand, in-situ Arctic SIT observations are rather scarce and localized, which can be hardly used for assimilation due to their limited spatial representation within a relatively large model grid cell.

In a recent study, Dawson et al. (2022) presented the first estimate of pan-Arctic summer sea-ice freeboard from radar altimeter by using a 1D convolutional neural network (CNN) to distinguish ice leads from melt ponds. Landy et al. (2022) converted summer CryoSat-2 radar freeboard to SIT and applied further corrections. The spring predictability barrier of the Arctic sea ice (e.g., Day, Tietsche, & Hawkins, 2014; Bushuk et al., 2017) suggests that sea-ice forecast should benefit from the initialization with SIT in the melt season (Bushuk et al., 2020). Therefore, it presents an opportunity to explore the extent to which the summer SIT observation could improve the real-time forecast skill. Min et al. (2023) demonstrated that assimilation of summer SIT corrects the overestimation in the Combined Model and Satellite Thickness (CMST; Mu et al., 2018b) product. Y.-F. Zhang et al. (2023) found that the assimilation of May to August CryoSat-2 SIT anomalies improves local SIC and sea-ice extent (SIE) forecasts in September. However, the influence of assimilating summer CryoSat-2 SIT observations on short-term sea-ice forecast in summer and on long-term forecast extending beyond September still needs further investigation.

In this study, we focus on the impact of summer SIT observations on the daily and seasonal forecast skills of a sea-ice prediction modelling system. In particular, we perform a series of short- and long-term ensemble sea-ice forecasts where the sea ice-ocean initial state is constrained by the summer CryoSat-2 SIT or where these data are not used. The benefits and challenges of using these new SIT data are evaluated and critically discussed using independent sea-ice data.

2 Data and Methods

2.1 The coupled sea ice-ocean model

We use a regional coupled sea ice-ocean model driven by atmospheric forecasts to configure the sea ice-ocean forecast system. The model is based on the Massachusetts Institute of Technology general circulation model (MITgcm; Marshall et al., 1997) and covers the pan-Arctic region with a horizontal resolution of around 18 km as in Losch et al. (2010). The sea-ice model uses a viscous-plastic rheology (Hibler III, 1979; J. Zhang & Hibler III, 1997) and a zero-layer thermodynamic formulation without heat capacity (Semtner, 1976; Parkinson & Washington, 1979). The readers are referred to Losch et al. (2010) and Nguyen et al. (2011) for more details on the model.

2.2 Data assimilation and forecast

The summer data assimilation system is initialized from restart files generated by CMST (Mu et al., 2018b) simulation with 11 ensemble members. CMST combines model physics with information from remote-sensed SIT and SIC observations. It successfully reproduces the spatio-temporal sea-ice variations (Mu et al., 2018b). In this study, the summer data assimilation and forecast strategy follows Mu et al. (2019). All observations and corresponding uncertainties are interpolated onto the 18-km model grid for assimilation. After the assimilation of sea-ice observations using a Local Error Subspace Transform Kalman Filter (Nerger et al., 2012) coded within the Parallel Data Assimilation Framework (Nerger et al., 2005), the ensemble sea-ice forecasts start from the new analyses and are integrated forced by the atmospheric forecasts (cf. Section 2.3). More details on the data assimilation and forecast system are given in Supporting Information.

The 80-km-resolution CryoSat-2 summer SIT data set is derived from local variations in the CryoSat-2 radar echo response using a deep learning method (Dawson et al., 2022; Landy et al., 2022). This is the first estimate of pan-Arctic summer SIT from satellite observations. The summer SIT is assimilated into the system on a daily basis using the observations linearly interpolated between two biweekly (twice per month) records. However, the roughness-induced electromagnetic range bias on the heavily-deformed ice in the coast regions leads to significant SIT underestimate north of the CAA and Greenland in late summer (Landy et al., 2022). Practically we set the observation uncertainties higher than the original values over thick ice regions, while still using the provided errors over thin ice regions (Supporting Information). The SIC data used in the assimilation are computed at the French Research Institute for Exploitation of the Sea (IFREMER) based on the 85-GHz SSM/I and SSM/IS channels with a resolution of 12.5 km (Kaleschke et al., 2001; Spreen et al., 2008; Kern et al., 2010). The uncertainty of the SIC observation is set to a constant value of 0.25 following Yang, Losa, Losch, Jung, and Nerger (2015).

The short-term ensemble assimilation and forecast experiments are driven by the 174-hour atmospheric ensemble forecasts from the United Kingdom Met Office (UKMO) Ensemble Prediction System (EPS; Bowler et al., 2008). For the long-term prediction, the ensemble members are driven by deterministic atmospheric forcing (single member). The atmospheric forecasts from the NCEP Climate Forecast System Version 2 (CFSv2; Saha et al., 2014) are used for the 9-month long-term forecasts, while the ECMWF Reanalysis v5 (ERA5; Hersbach et al., 2020) is used as the atmospheric forcing during the data assimilation to minimize the potential error caused by deviations of atmospheric forcing during this period.

2.3 Experiment design

In order to investigate the potential impact of the CryoSat-2 summer SIT on sea-ice forecasts, this study designs both short-term (7 days) and long-term (270 days) forecasts (Table. 1). These experiments are conducted over different months. The short-term experiments in 2015, which cover the melt season, start from the CMST restart files on May 1, May 31, June 30, July 30, and August 29, respectively. Each forecast experiment lasts for 30 days and on each day a 7-day sea-ice forecast is run using the atmospheric forcing from the daily UKMO ensemble forecasts. No data assimilation is applied in the control run of the short-term forecasts (Short-CTRL). The Short-SIT experiments assimilate only the CryoSat-2 summer SIT data, and the Short-SIC experiments assimilate only the SSMI/SSMIS SIC data, while both data sets are assimilated in the Short-SICSIT experiments. For the 2016 experiments, only the start dates are changed to match the available restart files from CMST (Table. 1).

The long-term forecast experiments are designed to diagnose the persistence of the assimilated CryoSat-2 summer SIT over the months from the melt season to the freezing season. The Long-SIT, Long-SIC and Long-SICSIT experiments with data assimilation start each summer month from CMST restart files. Unlike the incremental analysis update approach, the state vector is updated each day directly in the next 15 days to assimilate observations. Over that period, ERA5 atmospheric reanalysis forcing is used. Then, the 270-day sea-ice forecasts start from the sea-ice analysis restart files and are forced by the CFSv2 operational atmospheric forecasts. No data assimilation is performed in the Long-CTRL experiments. The forecast start dates are listed in Table 1.

2.4 Verification

Airborne electromagnetic SIT observations north of Greenland from AWI IceBird campaigns in July and August 2016 are employed for comparison with the assimilation results. Locations of these observations are indicated in Figure S1. The integrated ice-edge error (IIEE; Goessling et al., 2016) is used to quantify the skill of the short-term ice-edge forecasts. It measures the discrepancy between the forecasted and observed SIE. The reference observation used in this study is the 25-km-resolution NOAA/NSIDC Climate Data Record (CDR) of Passive Microwave Sea Ice Concentration Version 4 (Meier et al., 2021).

To validate the skill of the long-term sea-ice forecast, we compute the IIEE and the RMSD of SIT against various other products and in-situ observations. The IIEE is still computed using the NOAA/NSIDC CDR data. The RMSDs of SIT are computed with respect

Table 1. Summary of forecast experiments design. The number in the parenthesis represents the size of atmospheric forcing ensemble. Short: short-term forecast. Long: long-term forecast. SIC: sea-ice concentration. SIT: sea-ice thickness.

Experiment	Assimilated data	Forecast duration (days)	Atmospheric forcing during assimilation	Atmospheric forcing during forecast	Forecast start date
Short-CTRL	/	7	UKMO (11)	UKMO (11)	Daily forecast starting from 01 May 2015, 31 May 2015, 30 Jun 2015, 30 Jul 2015, 29 Aug 2015, 25 Apr 2016, 25 May 2016, 24 Jun 2016, 24 Jul 2016, 23 Aug 2016.
Short-SIT	CryoSat-2 SIT	7	UKMO (11)	UKMO (11)	
Short-SIC	SSMI/SSMIS SIC	7	UKMO (11)	UKMO (11)	
Short-SICSIT	SSMI/SSMIS SIC and CryoSat-2 SIT	7	UKMO (11)	UKMO (11)	
Long-CTRL	/	270	ERA5 (1)	CFSv2 (1)	16 May 2015, 15 Jun 2015, 15 Jul 2015, 14 Aug 2015, 13 Sep 2015, 10 May 2016, 09 Jun 2016, 09 Jul 2016, 08 Aug 2016, 07 Sep 2016.
Long-SIT	CryoSat-2 SIT	270	ERA5 (1)	CFSv2 (1)	
Long-SIC	SSMI/SSMIS SIC	270	ERA5 (1)	CFSv2 (1)	
Long-SICSIT	SSMI/SSMIS SIC and CryoSat-2 SIT	270	ERA5 (1)	CFSv2 (1)	

to the 25-km-resolution CS2SMOS products (Ricker et al., 2017) when they are available between October and the following April. Both NOAA/NSIDC CDR and CS2SMOS data are interpolated onto the 18-km grid to calculate the IIEE and RMSD. Note that CS2SMOS is a merged product using winter Cryosat-2 and Soil Moisture Ocean Salinity (SMOS) SIT. The SIT observations derived from upward-looking sonar moorings maintained by the Beaufort Gyre Exploration Program (BGEP) are used for the forecast evaluation. The three moorings BGEP-A, BGEP-B, and BGEP-D, which provide year-round sea-ice draft observations, are located at (75.0°N, 150.0°W), (78.0°N, 150.0°W) and (74.0°N, 140.0°W), respectively (Figure S1). The draft is converted to SIT by multiplying it by a constant factor of 1.1 as in Nguyen et al. (2011).

3 Result

3.1 Short-term ice-edge forecast

SIT from CryoSat-2 and the short-term experiments in 2015 is shown in Figure 1. The spatially averaged SIT differences between Short-SIT and Short-CTRL from May to September 2015 are 0.10 m, -0.06 m, -0.37 m, -0.37 m and -0.39 m, respectively. Overall, the SIT differences are smallest in May and June, when the assimilation of the summer CryoSat-2 observations reduces the SIT in the Pacific sector and increases it in the Atlantic sector (regions shown in Figure S1). Along with higher uncertainties in the CryoSat-2 SIT observations due to strong ice melting in July, August and September, a remarkable SIT reduction over the multi-year ice regions (regions shown in Figure S2) is found. SIT is also reduced in most of the marginal ice zones, especially in the Beaufort Sea and the Chukchi Sea. In our experiment, SIC assimilation, however, has only limited impact on SIT near the ice edge due to reliable restart states from CMST system that already has assimilated SIC observations. The absolute spatially averaged SIT differences between Short-SIC and Short-CTRL are minor, within 0.04 m. In the sea ice interior region with SIC close to 1.0 far from the ice edge, SIC assimilation can hardly further improve the SIT there by means of the covariance matrix, due to a narrow SIC ensemble spread. Similar results are also found in 2016 (Figure S3).

Assimilating summer CryoSat-2 SIT in Short-SIT gives rise to a more reasonable SIT probability density distribution along the trajectories of the IceBird campaigns north of Greenland (Figure S4), particularly for the modal SIT. Overestimation in CMST as indicated by Short-CTRL is significantly reduced. The median SIT difference against IceBird observations is mitigated in Short-SIT (-0.42 m), while it is -0.71 m and 0.98 m for CryoSat-2 and Short-SIC, respectively. Short-SIT removes ice thicker than 3 m, resulting in a lower median than IceBird observations. Compared to observations from BGEP moorings (Figure S5), the assimilation of summer CryoSat-2 SIT leads to a further underestimated SIT particularly in May, but corrects the SIT overestimation in late summer.

SIT assimilation has an important impact on SIC simulations through the physical connection between thickness and concentration over thin ice areas (Xie et al., 2016; Mignac et al., 2022). Short-term forecast of ice edge, defined as the 15% SIC isoline, can be strongly influenced by SIT assimilation. Figure 2 shows the IIEE difference in the Pacific sector and Atlantic sector (regions shown in Figure S1). IIEE in each forecast experiment is given in Figure S6. The observed SIC used as the reference for the IIEE calculation is the NOAA/NSIDC SIC CDR. The difference in the ice-edge position between forecasts and observations in 2015 and 2016 is displayed in Figure S7 and Figure S8.

The impact of CryoSat-2 SIT assimilation on ice-edge forecasts varies with time and region. Compared to Short-CTRL, IIEE in Short-SIT is strongly reduced in most times and both sectors (Figure 2). The ice-edge position in the forecasts is consistently overestimated in Short-CTRL. Assimilation of the summer SIT reduces the SIT of the forecasts near the

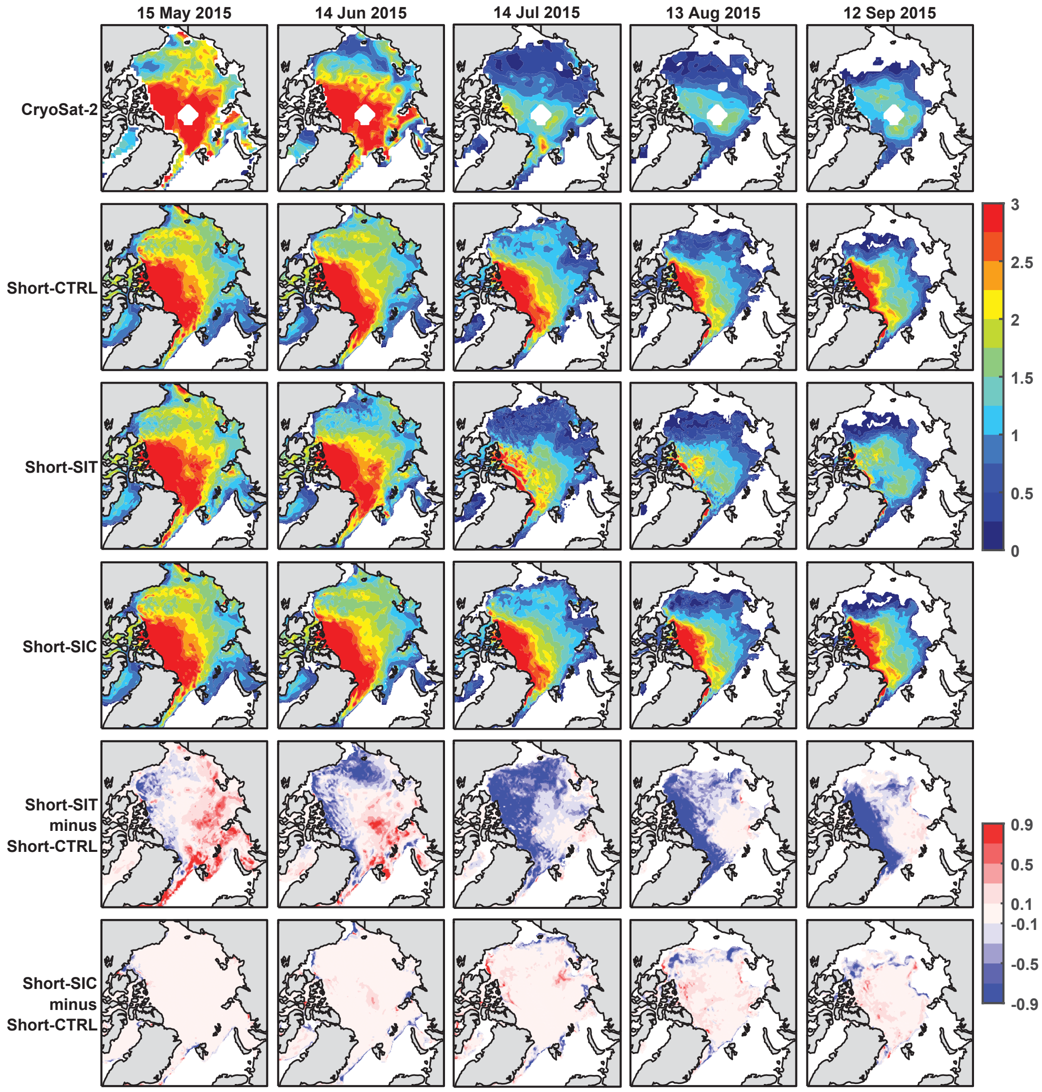

Figure 1. CryoSat-2 SIT (m) used for assimilation, SIT analysis from short-term experiments, and their differences between experiments on the 15th day from the model start date in 2015.

ice edge, resulting in a better agreement between the ice-edge forecasts and the ice-edge observations from the satellite compared with Short-CTRL (Figure S7 and Figure S8).

In the Pacific sector, only a slight improvement in IIEE is observed in May and June for Short-SIT compared to Short-CTRL (Figure 2). However, in July, especially in 2015, IIEE increases and the forecast skill degrades. This can be attributed to the fact that the melt-pond fraction starts to increase in June and reaches its maximum in July (Feng et al., 2022). In particular, 2015 was the peak year for observed melt-pond fraction in the Beaufort Sea between 2000-2021 (Xiong & Ren, 2023). The presence of excessive melt-pond fraction in this region may lead to more misclassification of ice leads and melt ponds in the CryoSat-2 sea-ice freeboard retrieval using the CNN model, which affects the SIT analysis in the Pacific sector. Therefore, the underestimated SIT erroneously leads to a large ice-edge error in July of the Short-SIT experiments. This warrants further refinement of the artificial intelligence algorithm used for summer CryoSat-2 SIT retrieval. In late summer, the assimilation of CryoSat-2 SIT observations in Short-SIT leads to more skillful ice-edge forecasts, resulting in a statistically significant average reduction in IIEE of about $2.1\times10^5\,\mathrm{km}^2$. For example, the assimilation of SIT allows the model to predict an ice-free "cave" inside the Beaufort Sea in August 2015, while it is completely covered by sea ice in Short-CTRL and still with a connected strip of ice in Short-SIC (Figure S7). Furthermore, the ice-edge forecasts in the Atlantic sector are also improved for Short-SIT compared to Short-CTRL, especially in June (about $0.8\times10^5\,\mathrm{km}^2$) and July (more than $0.9\times10^5\,\mathrm{km}^2$).

We further investigate the influences of SIC assimilation together with summer SIT assimilation on the ice-edge forecasts, considering the more important role of SIC observations on summer sea-ice forecasts as documented in the literature (e.g., Posey et al., 2015; Yang, Losa, Losch, Liu, et al., 2015). Forecasts from the Short-SICSIT experiments are also compared to the Short-SIC experiments, which performs SIC assimilation only.

In the Pacific sector, the additional SIT assimilation tends to yield more favorable ice-edge forecasts compared to Short-SIC (Figure 2). Similar to the IIEE differences between Short-SIT and Short-CTRL, the improvement in May and June between Short-SICSIT and Short-SIC is relatively small (only $3.0\times10^3\,\mathrm{km}^2$ on average). In July, IIEE becomes smaller in 2015 but larger in 2016 relative to Short-SIC. In late summer, the analysis of summer SIT observations significantly reduces the IIEE, bringing the ice-edge forecasts closer to the observations. In the Atlantic Sector, Short-SICSIT tends to give rise to larger IIEE, resulting in more detrimental effects, particularly noticeable in May and June (Figure 2). Nevertheless, these mean IIEE differences are still in the range of $\pm0.5\times10^5\,\mathrm{km}^2$, which is much smaller than the changes between Short-SIT and Short-CTRL. In the Atlantic sector, Short-SIC is already close to the observations due to a reasonable CMST SIT estimate north of the Svalbard and Novaya Zemlya, so further improvements are rather limited.

Note that, as illustrated by the solid lines representing the mean IIEE differences in Figure 2, the impact of the summer CryoSat-2 SIT assimilation becomes more obvious with increasing lead time in Short-SICSIT. The improvements of Short-SICSIT relative to Short-SIC increase as forecast progressing, while the deteriorations of IIEE become smaller, with the exception of the June 2016 forecasts.

3.2 Long-term sea-ice forecast

The Long-SIT experiments with summer CryoSat-2 SIT assimilation provides significant benefits for ice-edge and thickness forecasts against Long-CTRL. Reductions in IIEE are found for the first 30 days in May, June and August of 2015 and 2016 (Figure S9a, b). For experiments also initialized with SIC constraints, the IIEEs are reduced for most of the time during these three months, but not overall (Figure 3a, b). For the forecast initialized in July, the CryoSat-2 SIT assimilation is generally detrimental and only effective for a few days due to the underestimated thickness uncertainties caused by melt ponds. In September, improvements in ice-edge forecasts without SIC assimilation are seen for the first three weeks in 2015, and two weeks in 2016 (Figure S9a, b). The assimilation of SIC reduces such benefit (Figure 3a, b), which is not surprised.

With respect to the CS2SMOS SIT product, the predicted Arctic-wide thickness is also improved (Figure 3c, d; Figure S9c, d), except for the forecast starting in July 2016, which degrades after 140 days. The summer CryoSat-2 SIT mitigates the SIT overestimation in the Beaufort Sea in Long-CTRL and Long-SIC (not shown). The improvements are most pronounced in October, when the freezing season begins, and decrease exponentially with time until the forecast system falls into the control of the internal variability. This superior skill may even persist throughout the freezing season, similar to the previous findings on an optimal winter SIT initialization improving the predictive skill of summer sea ice (Blockley & Peterson, 2018). Consistent with the performance of the short-term forecasts in section 3.1, the reduction of SIT RMSD in 2015 is more significant than that in 2016. When SIC assimilation is absent, the effect of SIT initialization on ice-edge forecasts is more pronounced

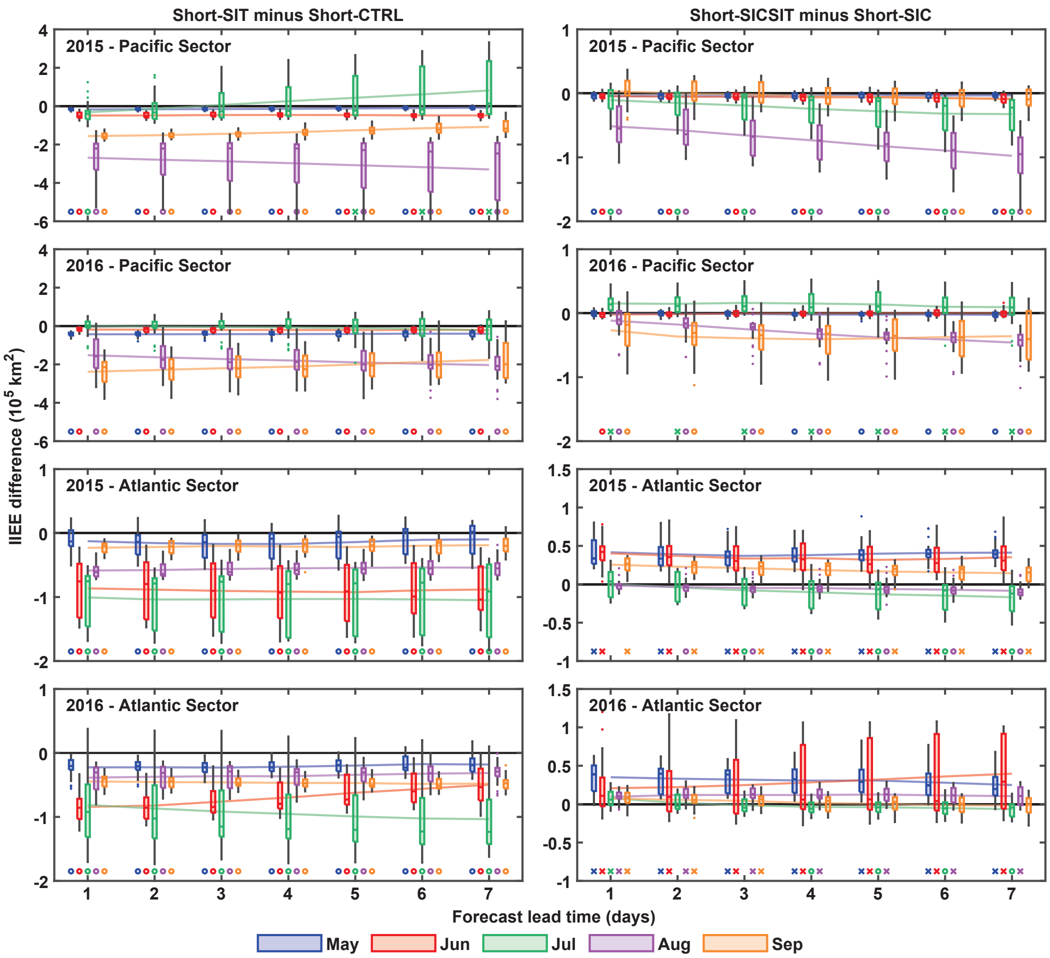

Figure 2. Box plot of the IIEE difference (10^5 km^2) between Short-SIT and Short-CTRL (left), together with that between Short-SICSIT and Short-SIC (right) in the 7-day sea-ice forecasts. The IIEE in the box plot is calculated after 7 days of assimilation when the summer CryoSat-2 SIT is fully assimilated. Box colors indicate different months. Box sizes indicate IIEE difference between the lower and upper quartiles. Outliers denote values more than 1.5 interquartile range from the top or bottom of the colored box. The outer edges of the black lines denote the minimum and maximum values that are not outliers. Solid-colored lines show the mean IIEE difference at each lead time. A positive value indicates an increase in IIEE, when SIT is assimilated, while a negative value indicates a decrease in the IIEE. Markers at the bottom of each panel indicate increases (cross) and decreases (circle) in IIEE that pass the Student's T-test at the 95% confidence level. Negative values indicate better forecast skills. Note that different subfigures use different y-axis scales.

(Figure S9). However, the skill of the long-term SIT forecasts remains nearly unchanged regardless of whether SIC assimilation is included.

We also examine the performance of the long-term SIT forecasts at the BGEP sites (Figure S5). In general, significant improvements in the SIT forecasts are found in Long-SICSIT initialized in July, August and September of 2015. The differences between Long-SICSIT and Long-SIC in 2016 are limited, not exceeding 30 cm most of the time. The forecasts tend to overestimate SIT in the early freezing season in the Beaufort Sea. To check if these biases are caused by the growing errors in the long-term atmospheric forecasts, we performed additional forecast experiments in 2015 with the same configuration as Long-CTRL, except that the CFSv2 atmospheric forecast is replaced by the ERA5 reanalysis for the atmospheric forcing. The ERA5 driven simulations show a similar overestimation of SIT in the Beaufort Sea (not shown). The anticyclonic wind in the Beaufort Gyre pushes excessively thick ice from the multi-year ice region north of the CAA into the Beaufort Sea. This suggests that the overestimation is not mainly due to biases in the atmospheric forcing but imperfect model parameterizations and initial ice-ocean conditions.

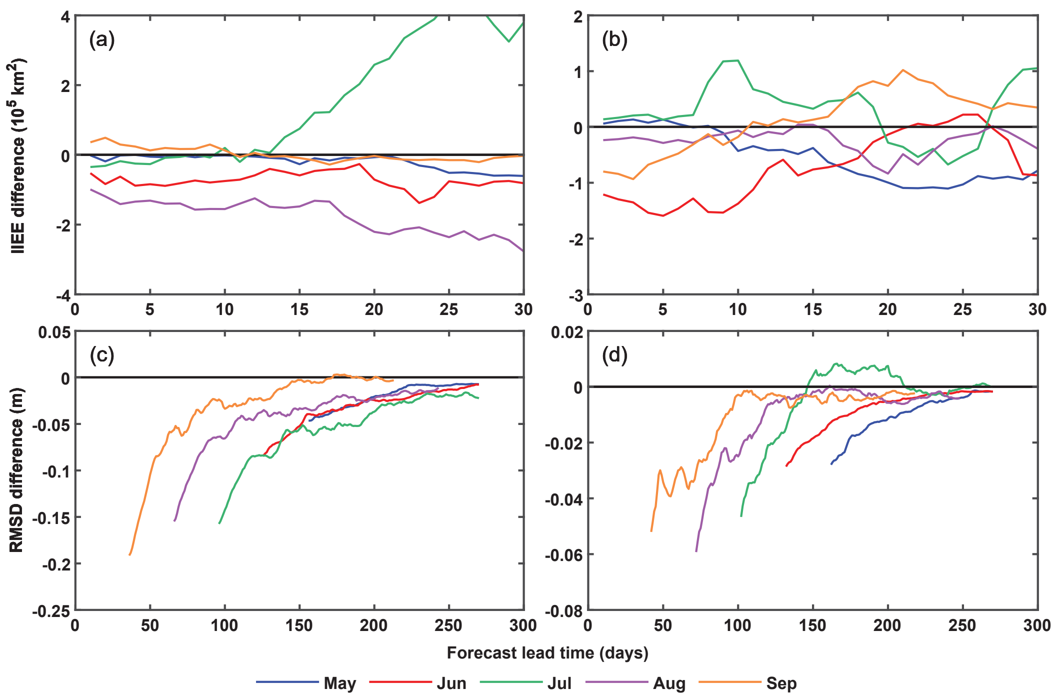

Figure 3. The difference of the IIEE (10^5 km^2) in 2015 (a) and in 2016 (b), and the difference of the SIT RMSD (m) in 2015 (c) and in 2016 (d) between Long-SICSIT and Long-SIC forecasts initialized from May to September (Long-SICSIT minus Long-SIC). The RMSD of the SIT is computed with respect to the CS2SMOS product available from October to April for (c) and (d). Negative values indicate better forecast skill. Note that different subfigures use different y-axis scales.

4 Summary

This study examines the impact of summer CryoSat-2 SIT assimilation on short- and long-term sea-ice forecasts in 2015 and in 2016. Compared to the experiments without any data assimilation, the ice-edge forecasts with summer CryoSat-2 SIT assimilation are improved. When the summer CryoSat-2 SIT data are assimilated together with SIC data, the effects on the ice-edge forecast skill are rather dependent on the time when the forecast is initialized and are spatially highly variable. In the Pacific sector, the combined assimilation of summer SIT and SIC observations leads to more realistic summer ice-edge forecasts with a one-week lead time.

The long-term sea-ice forecasts show significant reductions in both IIEE and RMSD of the SIT, except for those initialized in July, when the summer CryoSat-2 SIT has large uncertainties. The improvement in ice-edge forecasts can last up to about 30 days, while for the SIT forecasts the benefits can last for more than 3 months. This result demonstrates that, although the atmospheric forecasts used to drive the model can evolve freely after about one month, the SIT initialization in summer remains a primary factor in predicting long-term SIT variations. An extended study covering all available years of the CryoSat-2 dataset may concrete the conclusion.

However, limitations of the summer CryoSat-2 SIT data product still remain. The deep learning algorithm used has a certain degree of uncertainty in classifying ice leads and melt ponds, especially when the melt-pond fraction is large. The underestimation in the summer CryoSat-2 SIT from July to September in the coastal regions north of the CAA and Greenland requires further work on the sea-ice freeboard and thickness retrieval algorithm or exploration of new correction schemes to improve their reliability and accuracy. Furthermore, it is still an open question how this product should be used for real-time Arctic sea-ice forecasting, since its uncertainty currently does not account for all the algorithm errors, and possible representation errors (Janjić et al., 2018) should be considered accurately.

5 Open Research

The ensemble mean Arctic sea-ice thickness (SIT) and sea-ice concentration (SIC) forecast data used in the study can be downloaded at Song et al. (2024). The file size of the forecast results with all ensemble members exceeds 50GB and can be made available upon request through contact. The CMST SIT estimate is available at Mu et al. (2018a). The summer CryoSat-2 SIT observations can be downloaded from Landy and Dawson (2022). The SSMI/SSMIS SIC data is avaliable from Kern et al. (2024). The UKMO atmospheric ensemble forecasts are avaliable in the THORPEX Interactive Grand Global Ensemble (TIGGE; Bougeault et al., 2010) archive (`https://apps.ecmwf.int/datasets/data/tigge`). The hourly ERA5 reanalysis is avaliable at Hersbach et al. (2023). The CFSv2 atmospheric forecasts are avaliable at `https://www.ncei.noaa.gov/products/weather-climate-models/climate-forecast-system`. The NOAA/NSIDC SIC CDR data is available at Meier et al. (2021). The CS2SMOS data is avaliable at `https://www.meereisportal.de`. Mooring observations from BGEP are downloaded from `https://www2.whoi.edu/site/beaufortgyre`. The EASE-Grid Sea Ice Age, Version 4 (Tschudi et al., 2019) is avaliable at `https://nsidc.org/data/nsidc-0611/versions/4`.

Acknowledgments

We thank two anonymous reviewers for their constructive comments. We thank Thomas Krumpen for providing sea ice thickness observations from AWI IceBird campaigns. This study is supported by the National Key R&D Program of China under Grant 2019YFA0607000, the National Natural Science Foundation of China (42176235) and the computing resources supported by the Laoshan Laboratory (LSKJ202202301, LSKJ202300303). Contribution of Svetlana N. Loza was supported by the Federal Ministry of Education and Research of Germany in the framework of the Seamless Sea Ice Prediction project (SSIP, Grant 01LN1701A) and partly made in the framework of the state assignment of SIO RAS (theme FMWE-2024-0028).

References

Blanchard-Wrigglesworth, E., Bitz, C. M., & Holland, M. M. (2011, 09). Influence of initial conditions and climate forcing on predicting arctic sea ice. *Geophysical Research Letters*, *38*, L18503. doi: 10.1029/2011GL048807

Blockley, E. W., & Peterson, K. A. (2018). Improving met office seasonal predictions of arctic sea ice using assimilation of cryosat-2 thickness. *The Cryosphere*, *12*(11), 3419-3438. doi: 10.5194/tc-12-3419-2018

Bougeault, P., Toth, Z., Bishop, C., Brown, B., Burridge, D., Chen, D. H., … Worley,

S. (2010). The thorpex interactive grand global ensemble. *Bulletin of the American Meteorological Society*, *91*(8), 1059-1072. doi: 10.1175/2010BAMS2853.1

Bowler, N. E., Arribas, A., Mylne, K. R., Robertson, K. B., & Beare, S. E. (2008). The mogreps short–range ensemble prediction system. *Quarterly Journal of the Royal Meteorological Society*, *134*(632), 703–722. doi: 10.1002/qj.234

Bushuk, M., Msadek, R., Winton, M., Vecchi, G. A., Gudgel, R., Rosati, A., & Yang, X. (2017). Skillful regional prediction of arctic sea ice on seasonal timescales. *Geophysical Research Letters*, *44*(10), 4953-4964. doi: 10.1002/2017GL073155

Bushuk, M., Winton, M., Bonan, D. B., Blanchard-Wrigglesworth, E., & Delworth, T. L. (2020). A mechanism for the arctic sea ice spring predictability barrier. *Geophysical Research Letters*, *47*(13), e2020GL088335. doi: 10.1029/2020GL088335

Bushuk, M., Zhang, Y., Winton, M., Hurlin, B., Delworth, T., Lu, F., … Zeng, F. (2022, 07). Mechanisms of regional arctic sea ice predictability in two dynamical seasonal forecast systems. *Journal of Climate*, *35*, 4207-4231. doi: 10.1175/JCLI-D-21-0544.1

Comiso, J. C., Parkinson, C. L., Gersten, R., & Stock, L. (2008). Accelerated decline in the arctic sea ice cover. *Geophysical Research Letters*, *35*(1), L01703. doi: 10.1029/2007GL031972

Dawson, G., Landy, J., Tsamados, D. M., Komarov, A. S., Howell, S., Heorton, H., & Krumpen, T. (2022, 01). A 10-year record of arctic summer sea ice freeboard from cryosat-2. *Remote Sensing of Environment*, *268*, 112744. doi: 10.1016/j.rse.2021.112744

Day, J. J., Hawkins, E., & Tietsche, S. (2014). Will arctic sea ice thickness initialization improve seasonal forecast skill? *Geophysical Research Letters*, *41*, 7566-7575. doi: 10.1002/2014GL061694

Day, J. J., Tietsche, S., & Hawkins, E. (2014). Pan-arctic and regional sea ice predictability: initialization month dependence. *Journal of Climate*, *27*(12), 4371-4390. doi: 10.1175/JCLI-D-13-00614.1

Dirkson, A., Merryfield, W. J., & Monahan, A. H. (2017). Impacts of sea ice thickness initialization on seasonal arctic sea ice predictions. *Journal of Climate*, *30*, 1001-1017. doi: 10.1175/JCLI-D-16-0437.1

Drinkwater, M. R. (1991). K $_u$ band airborne radar altimeter observations of marginal sea ice during the 1984 marginal ice zone experiment. *Journal of Geophysical Research: Oceans*, *96*(C3), 4555-4572. doi: 10.1029/90JC01954

Feng, J., Zhang, Y., Cheng, Q., & Tsou, J. Y. (2022). Pan-arctic melt pond fraction trend, variability, and contribution to sea ice changes. *Global and Planetary Change*, *217*, 103932. doi: 10.1016/j.gloplacha.2022.103932

Goessling, H. F., Tietsche, S., Day, J. J., Hawkins, E., & Jung, T. (2016). Predictability of the arctic sea-ice edge. *Geophysical Research Letters*, *43*, 1642–1650. doi: 10.1002/2015GL067232

Guemas, V., Blanchard-Wrigglesworth, E., Chevallier, M., Day, J. J., Déqué, M., Doblas-Reyes, F. J., … Tietsche, S. (2016). A review on arctic sea ice predictability and prediction on seasonal-to-decadal timescales. *Quarterly Journal of the Royal Meteorological Society*, *142*, 546-561. doi: 10.1002/qj.2401

Hebert, D. A., Allard, R. A., Metzger, E. J., Posey, P. G., Preller, R. H., Wallcraft, A. J., … Smedstad, O. M. (2015, 11). Short-term sea ice forecasting: An assessment of ice concentration and ice drift forecasts using the u.s. navy's arctic cap nowcast/forecast system. *Journal of Geophysical Research: Oceans*, *120*, 8327-8345. doi: 10.1002/2015JC011283

Hersbach, H., Bell, B., Berrisford, P., Biavati, G., Horányi, A., Muñoz Sabater, J., … Thépaut, J.-N. (2023). *Era5 hourly data on single levels from 1940 to present* [dataset]. Copernicus Climate Change Service (C3S) Climate Data Store (CDS). Retrieved from `https://cds.climate.copernicus.eu/cdsapp#!/dataset/reanalysis-era5-single-levels?tab=overview` doi: 10.24381/cds.adbb2d47

Hersbach, H., Bell, B., Berrisford, P., Hirahara, S., Horányi, A., Muñoz-Sabater, J., … Thépaut, J.-N. (2020). The era5 global reanalysis. *Quarterly Journal of the Royal*

Meteorological Society, 1999–2049. doi: 10.1002/qj.3803

Hibler III, W. D. (1979). A dynamic thermodynamic sea ice model. *Journal of Physical Oceanography*, *9*, 815-846. doi: 10.1175/1520-0485(1979)009⟨0815:ADTSIM⟩2.0.CO;2

Janjić, T., Bormann, N., Bocquet, M., Carton, J. A., Cohn, S. E., Dance, S. L., ... Weston, P. (2018). On the representation error in data assimilation. *Quarterly Journal of the Royal Meteorological Society*, *144*(713), 1257-1278. doi: 10.1002/qj.3130

Jung, T., Gordon, N. D., Bauer, P., Bromwich, D. H., Chevallier, M., Day, J. J., ... Yang, Q. (2016). Advancing polar prediction capabilities on daily to seasonal time scales. *Bulletin of the American Meteorological Society*, *97*, 160113112747009. doi: 10.1175/BAMS-D-14-00246.1

Kaleschke, L., Lüpkes, C., Vilna, T., Haarpaintner, J., Borchert, A., Hartmann, J., & Heygster, G. (2001). Ssm/i sea ice remote sensing for mesoscale ocean-atmosphere interaction analysis. *Canadian Journal of Remote Sensing*, *27*, 526-537. doi: 10.1080/07038992.2001.10854892

Kern, S., Kaleschke, L., Girard-Ardhuin, F., Spreen, G., & Beitsch, A. (2024). *Global daily gridded 5-day median-filtered, gap-filled asi algorithm ssmi-ssmis sea ice concentration data* [dataset]. Integrated Climate Date Center. Retrieved from `https://www.cen.uni-hamburg.de/en/icdc/data/cryosphere/seaiceconcentration-asi-ssmi.html`

Kern, S., Kaleschke, L., & Spreen, G. (2010). Climatology of the nordic (irminger, greenland, barents, kara and white/pechora) seas ice cover based on 85 ghz satellite microwave radiometry: 1992–2008. *Tellus A*, *62*, 411-434. doi: 10.3402/tellusa.v62i4.15709

Kwok, R., & Rothrock, D. A. (2009). Decline in arctic sea ice thickness from submarine and icesat records: 1958-2008. *Geophysical Research Letters*, *36*, L15501. doi: 10.1029/2009GL039035

Landrum, L., & Holland, M. M. (2020, 12). Extremes become routine in an emerging new arctic. *Nature Climate Change*, *10*, 1-8. doi: 10.1038/s41558-020-0892-z

Landy, J. C., & Dawson, G. J. (2022). *Year-round arctic sea ice thickness from cryosat-2 baseline-d level 1b observations 2010-2020 (version 1.0)* [dataset]. NERC EDS UK Polar Data Centre. Retrieved from `https://data.bas.ac.uk/full-record.php?id=GB/NERC/BAS/PDC/01613` doi: 10.5285/d8c66670-57ad-44fc-8fef-942a46734ecb

Landy, J. C., Dawson, G. J., Tsamados, M., Bushuk, M., Stroeve, J. C., Howell, S. E. L., ... Aksenov, Y. (2022). A year-round satellite sea-ice thickness record from cryosat-2. *Nature*, *609*, 1-6. doi: 10.1038/s41586-022-05058-5

Laxon, S. W., Giles, K. A., Ridout, A. L., Wingham, D. J., Willatt, R., Cullen, R., ... Davidson, M. (2013). Cryosat-2 estimates of arctic sea ice thickness and volume. *Geophysical Research Letters*, *40*(4), 732-737. doi: 10.1002/grl.50193

Lee, S., Kim, H.-C., & Im, J. (2018). Arctic lead detection using a waveform mixture algorithm from cryosat-2 data. *The Cryosphere*, *12*(5), 1665-1679. doi: 10.5194/tc-12-1665-2018

Lemieux, J.-F., Beaudoin, C., Dupont, F., Roy, F., Smith, G. C., Shlyaeva, A., ... Ferry, N. (2015, 03). The regional ice prediction system (rips): Verification of forecast sea ice concentration. *Quarterly Journal of the Royal Meteorological Society*, *142*, 632-643. doi: 10.1002/qj.2526

Losch, M., Menemenlis, D., Campin, J.-M., Heimbach, P., & Hill, C. (2010). On the formulation of sea-ice models. part 1: Effects of different solver implementations and parameterizations. *Ocean Modelling*, *33*(1), 129-144. doi: 10.1016/j.ocemod.2009.12.008

Marshall, J., Adcroft, A., Hill, C., Perelman, L., & Heisey, C. (1997). A finite-volume, incompressible navier stokes model for studies of the ocean on parallel computers. *Journal of Geophysical Research*, *102*, 5753-5766. doi: 10.1029/96JC02775

Maykut, G. A., Grenfell, T. C., & Weeks, W. (1992). On estimating spatial and temporal variations in the properties of ice in the polar oceans. *Journal of Marine Systems*, *3*, 41-72. doi: 10.1016/0924-7963(92)90030-C

Meier, W. N., Fetterer, F., Windnagel, A. K., & Stewart., J. S. (2021). *Noaa/nsidc cli-*

mate data record of passive microwave sea ice concentration, version 4 [dataset]. National Snow and Ice Data Center. Retrieved from https://nsidc.org/data/G02202/versions/4 doi: 10.7265/efmz-2t65

Mignac, D., Martin, M., Fiedler, E., Blockley, E., & Fournier, N. (2022, 02). Improving the met office's forecast ocean assimilation model (foam) with the assimilation of satellite-derived sea-ice thickness data from cryosat-2 and smos in the arctic. *Quarterly Journal of the Royal Meteorological Society*, *148*, 1-24. doi: 10.1002/qj.4252

Min, C., Yang, Q., Luo, H., Chen, D., Krumpen, T., Mamnun, N., ... Nerger, L. (2023). Improving arctic sea-ice thickness estimates with the assimilation of cryosat-2 summer observations. *Ocean-Land-Atmosphere Research*, *2*, 0025. doi: 10.34133/olar.0025

Mu, L., Liang, X., Yang, Q., Liu, J., & Zheng, F. (2019). Arctic ice ocean prediction system: evaluating sea ice forecasts during xuelong's first trans-arctic passage in summer 2017. *Journal of Glaciology*, 1-9. doi: 10.1017/jog.2019.55

Mu, L., Losch, M., Yang, Q., Ricker, R., Losa, S. N., & Nerger, L. (2018a). *The arctic combined model and satellite sea ice thickness (cmst) dataset* [dataset]. PANGAEA. Retrieved from https://doi.org/10.1594/PANGAEA.891475 doi: 10.1594/PANGAEA.891475

Mu, L., Losch, M., Yang, Q., Ricker, R., Losa, S. N., & Nerger, L. (2018b). Arctic-wide sea ice thickness estimates from combining satellite remote sensing data and a dynamic ice-ocean model with data assimilation during the cryosat-2 period. *Journal of Geophysical Research: Oceans*, *123*, 7763-7780. doi: 10.1029/2018JC014316

Mu, L., Nerger, L., Streffing, J., Tang, Q., Niraula, B., Zampieri, L., ... Goessling, H. F. (2022). Sea-ice forecasts with an upgraded awi coupled prediction system. *Journal of Advances in Modeling Earth Systems*, *14*(12), e2022MS003176. doi: 10.1029/2022MS003176

Nerger, L., Hibler III, W. D., & SCHRÖTER, J. (2005). Pdaf-the parallel data assimilation framework: Experiences with kalman filtering. *World Scientific*, 63–83. doi: 10.1142/9789812701831_0006

Nerger, L., Janjić, T., Schröter, J., & Hiller, W. (2012). A regulated localization scheme for ensemble-based kalman filters. *Quarterly Journal of the Royal Meteorological Society*, *138*(664), 802-812. doi: 10.1002/qj.945

Nguyen, A. T., Menemenlis, D., & Kwok, R. (2011). Arctic ice-ocean simulation with optimized model parameters: Approach and assessment. *Journal of Geophysical Research: Oceans*, *116*, C04025. doi: 10.1029/2010JC006573

Parkinson, C. L., & Washington, W. M. (1979). A large-scale numerical model of sea ice. *Journal of Geophysical Research*, *84*, 311-337. doi: 10.1029/JC084iC01p00311

Posey, P., Metzger, E., Wallcraft, A., Hebert, D., Allard, R., Smedstad, O., ... Helfrich, S. (2015, 08). Improving arctic sea ice edge forecasts by assimilating high horizontal resolution sea ice concentration data into the us navy's ice forecast systems. *The Cryosphere*, *9*, 1735-1745. doi: 10.5194/tc-9-1735-2015

Ricker, R., Hendricks, S., Helm, V., Skourup, H., & Davidson, M. (2014). Sensitivity of cryosat-2 arctic sea-ice freeboard and thickness on radar-waveform interpretation. *The Cryosphere*, *8*, 1607-1622. doi: 10.5194/tc-8-1607-2014

Ricker, R., Hendricks, S., Kaleschke, L., Tian-Kunze, X., King, J., & Haas, C. (2017). A weekly arctic sea-ice thickness data record from merged cryosat-2 and smos satellite data. *The Cryosphere*, *11*(4), 1607–1623. doi: 10.5194/tc-11-1607-2017

Rothrock, D. A., Yu, Y., & Maykut, G. A. (1999). Thinning of the arctic sea-ice cover. *Geophysical Research Letters*, *26*, 3469-3472. doi: 10.1029/1999GL010863

Saha, S., Moorthi, S., Wu, X., Wang, J., Nadiga, S., Tripp, P., ... Becker, E. (2014). The ncep climate forecast system version 2. *Journal of Climate*, *27*, 2185–2208. doi: 10.1175/JCLI-D-12-00823.1

Semtner, A. J. (1976). A model for thermodynamic growth of sea ice in numerical investigations if climate. *Journal of Physical Oceanography*, *6*, 379-389. doi: 10.1175/1520-0485(1976)006⟨0379:AMFTTG⟩2.0.CO;2

Shu, Q., Qiao, F., Liu, J., Song, Z., Chen, Z., Zhao, J., ... Song, Y. (2021). Arctic sea ice concentration and thickness data assimilation in the fio-esm climate forecast system. *Acta Oceanologica Sinica*, *40*, 65-75. doi: 10.1007/s13131-021-1768-4

Song, R., Mu, L., Kauker, F., Loza, S., & Chen, X. (2024). *Forecast data for the paper: "assimilating summer sea-ice thickness observations improves arctic sea-ice forecast"* [dataset]. Zenodo. Retrieved from `https://doi.org/10.5281/zenodo.11352863` doi: 10.5281/zenodo.11352863

Spreen, G., Kaleschke, L., & Heygster, G. (2008). Sea ice remote sensing using amsr-e 89-ghz channels. *Journal of Geophysical Research*, *113*, C02S03. doi: 10.1029/2005JC003384

Stroeve, J. C., Serreze, M. C., Holland, M. M., Kay, J. E., Malanik, J., & Barrett, A. P. (2012, 02). The arctic's rapidly shrinking sea ice cover: A research synthesis. *Climatic Change*, *110*, 1005-1027. doi: 10.1007/s10584-011-0101-1

Tilling, R., Ridout, A., & Shepherd, A. (2019). Assessing the impact of lead and floe sampling on arctic sea ice thickness estimates from envisat and cryosat-2. *Journal of Geophysical Research: Oceans*, *124*, 7473–7485. doi: 10.1029/2019JC015232

Tschudi, M., Meier, W. N., J. S. Stewart, C. F., & Maslanik., J. (2019). *Ease-grid sea ice age, version 4* [dataset]. NASA National Snow and Ice Data Center Distributed Active Archive Center. Retrieved from `https://nsidc.org/data/NSIDC-0611/versions/4` doi: 10.5067/UTAV7490FEPB

Xie, J., Counillon, F., Bertino, L., Tian-Kunze, X., & Kaleschke, L. (2016). Benefits of assimilating thin sea ice thickness from smos into the topaz system. *The Cryosphere*, *10*, 2745–2761. doi: 10.5194/tc-10-2745-2016

Xiong, C., & Ren, Y. (2023). Arctic sea ice melt pond fraction in 2000–2021 derived by dynamic pixel spectral unmixing of modis images. *ISPRS Journal of Photogrammetry and Remote Sensing*, *197*, 181-198. doi: 10.1016/j.isprsjprs.2023.01.023

Yang, Q., Losa, S. N., Losch, M., Jung, T., & Nerger, L. (2015). The role of atmospheric uncertainty in arctic summer sea ice data assimilation and prediction. *Quarterly Journal of the Royal Meteorological Society*, *141*, 2314-2323. doi: 10.1002/qj.2523

Yang, Q., Losa, S. N., Losch, M., Liu, J., Zhang, Z., Nerger, L., & Yang, H. (2015). Assimilating summer sea-ice concentration into a coupled ice–ocean model using a lseik filter. *Annals of Glaciology*, *56*(69), 38–44. doi: 10.3189/2015AoG69A740

Zhang, J., & Hibler III, W. D. (1997). On an efficient numerical method for modeling sea ice dynamics. *Journal of Geophysical Research*, *102*, 8691–8702. doi: 10.1029/96JC03744

Zhang, Y.-F., Bushuk, M., Winton, M., Hurlin, B., Gregory, W., Landy, J., & Jia, L. (2023). Improvements in september arctic sea ice predictions via assimilation of summer cryosat-2 sea ice thickness observations. *Geophysical Research Letters*, *50*(24), e2023GL105672. doi: 10.1029/2023GL105672

Figure 1.

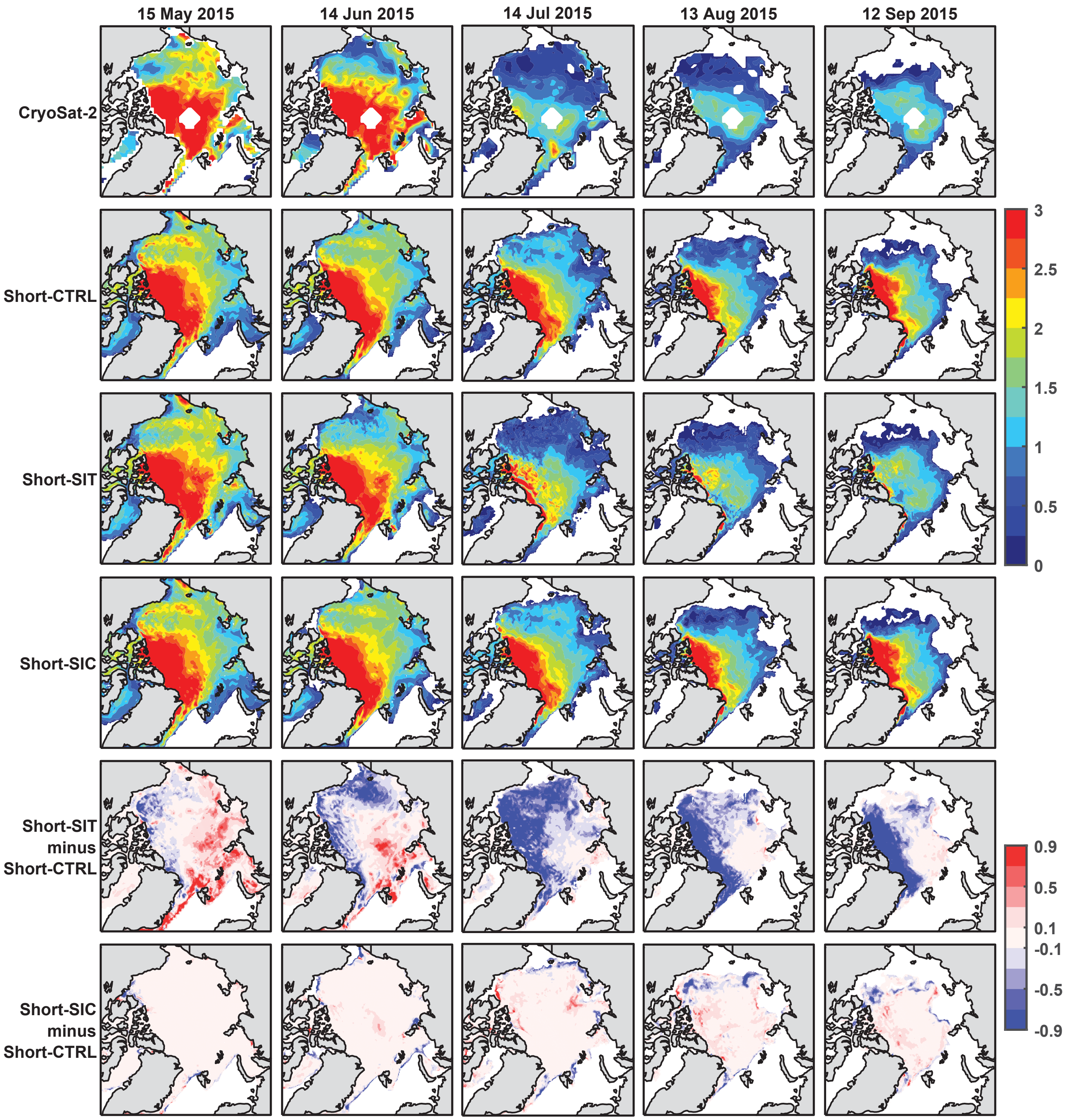

15 May 2015
14 Jun 2015
14 Jul 2015
13 Aug 2015
12 Sep 2015
CryoSat-2
Short-CTRL
Short-SIT
Short-SIC
Short-SIT minus Short-CTRL
Short-SIC minus Short-CTRL
3
2.5
2
1.5
1
0.5
0
0.9
0.5
0.1
-0.1
-0.5
-0.9

Figure 2.

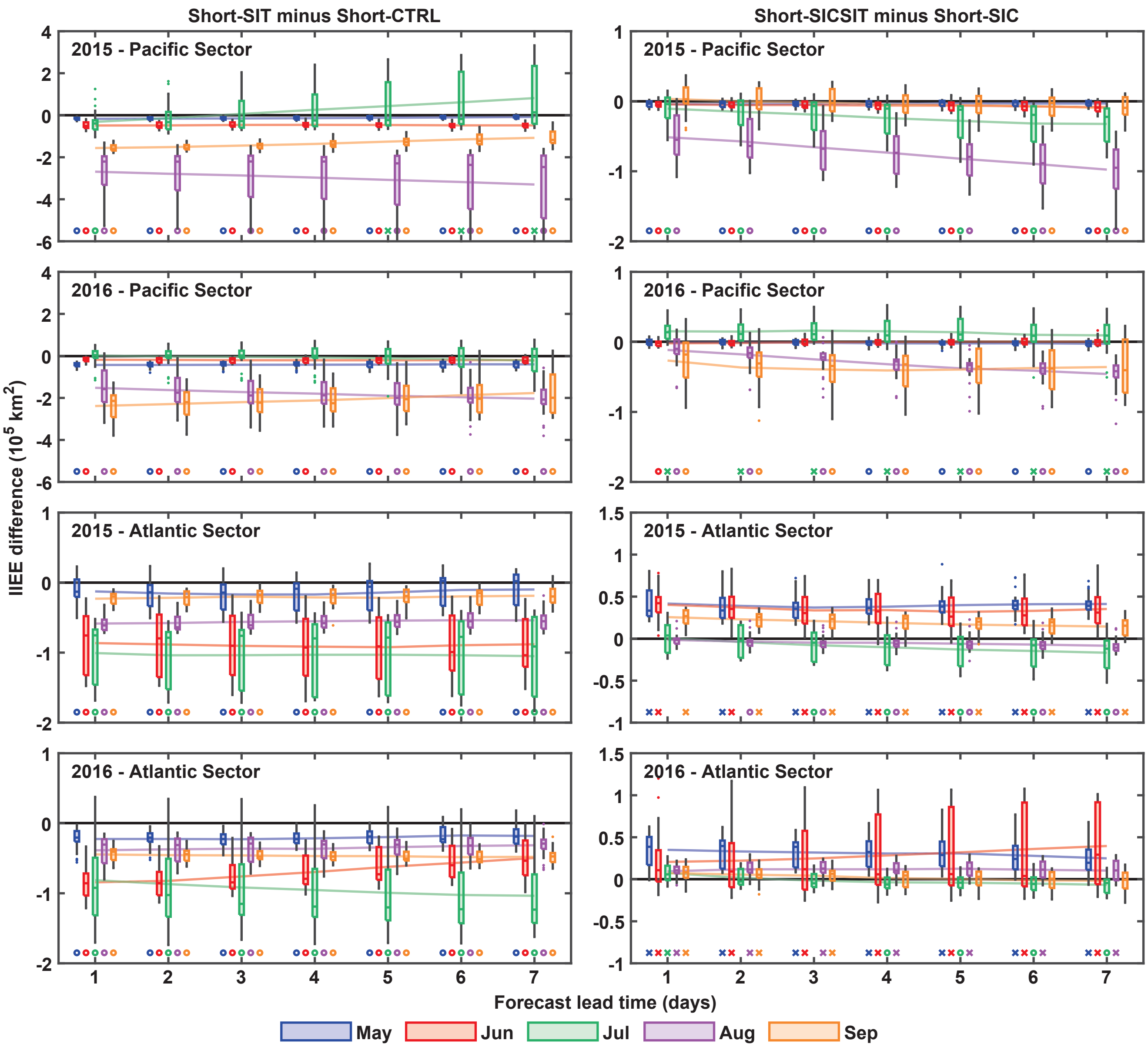

Short-SIT minus Short-CTRL
Short-SICSIT minus Short-SIC
2015 - Pacific Sector
2016 - Pacific Sector
2015 - Atlantic Sector
2016 - Atlantic Sector
IIEE difference (10^5 km^2)
Forecast lead time (days)
May
Jun
Jul
Aug
Sep

Figure 3.

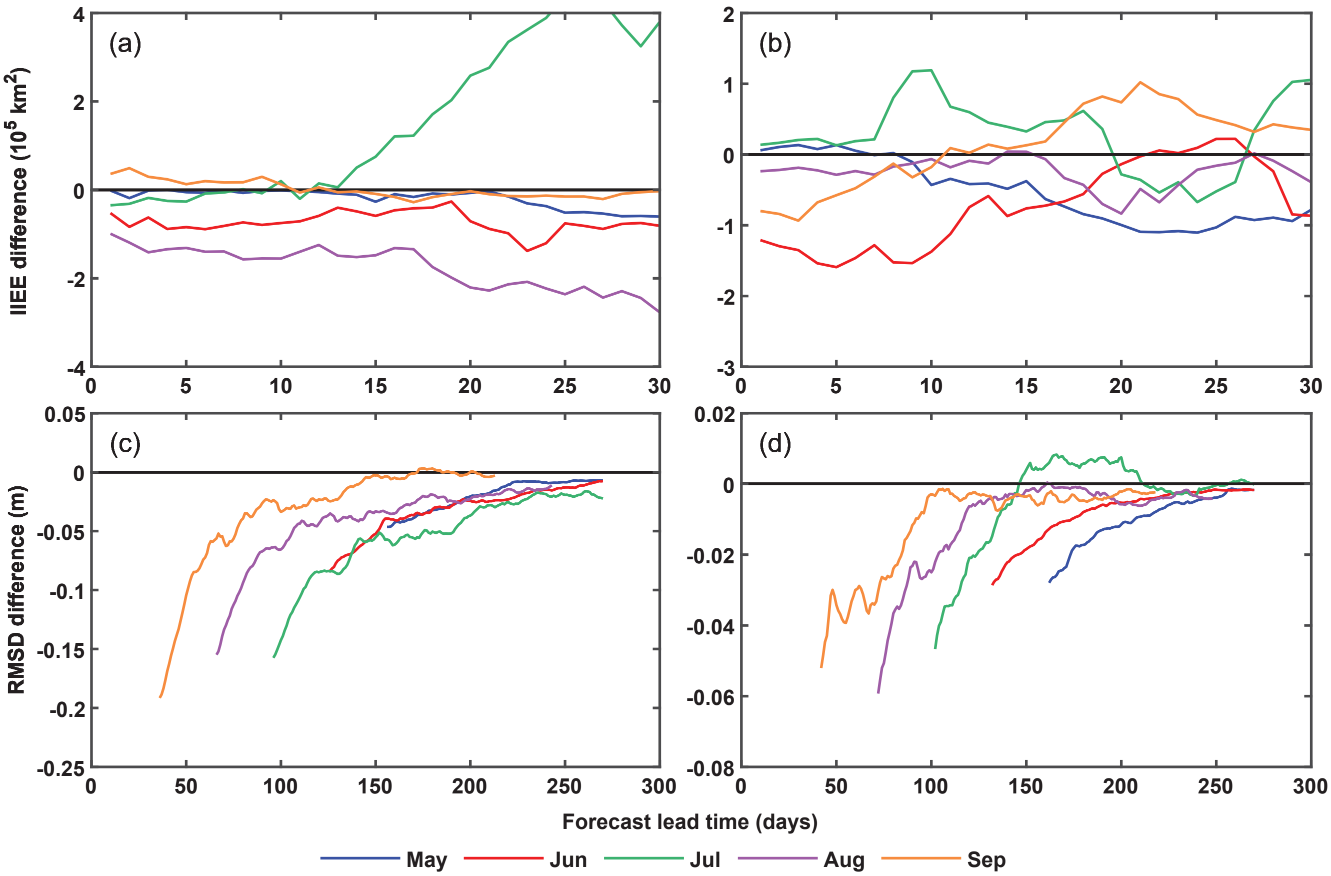

(a)
(b)
(c)
(d)
IIEE difference (10^5 km^2)
RMSD difference (m)
Forecast lead time (days)
May
Jun
Jul
Aug
Sep